Novel 2-Substituted Benzothiazole Derivatives: Synthesis, In-vitro and In- silico Evaluations as Potential Anticancer Agents

Rasha A. Azzam
Helwan University
Mona M. Seif
Helwan University
Maha A. El-Demellawy
The City of Scientific Research and Technological Applications (SRTA-City)
Galal H. Elgemeie
galal_elgemeie@science.helwan.edu.eg

Helwan University

Research Article

Keywords: Benzothiazoles, anticancer, in-silico, docking, PTK

Posted Date: May 6th, 2024

DOI: https://doi.org/10.21203/rs.3.rs-4298332/v1

Additional Declarations: No competing interests reported.

Abstract

Cancer remains a global health concern, demanding the development of new therapeutic medicines. This research focuses on the synthesis, *in vitro* evaluation, and *in silico* analysis of new 2-substituted benzothiazole derivatives as possible anticancer drugs. Hybrid molecules comprising benzothiazole and pyridinone rings **10a-d** and **14a-d** were also synthesized. Several compounds were produced and characterized, using NMR, IR and elemental analysis, with promising anticancer activity against lung H1299, liver Hepg2 and breast MCF7 cancer cell lines. Structure-activity connection investigations identified crucial structural characteristics that influence potency, with particular benzylidine derivatives **7a-g** demonstrating higher activity. *In-silico* ADME research revealed favorable drug-like features for chosen compounds, such as high gastrointestinal absorption and selective CYP inhibition. Toxicological projections indicated few side effects, confirming their potential as medication candidates. Docking studies revealed their binding mechanisms and interactions with protein tyrosine kinases PTK, identifying intriguing candidates for further study.

1. Introduction

Cancer is one of the deadliest diseases in the world, killing nearly 10 million people in 2020. When it comes to global mortality statistics, cancer is the second most common cause of death. The most prevalent causes of cancer mortality in 2020 are lung, colon, rectum, liver, stomach, and breast [1][2]. Over the last decade, cancer-related deaths have increased by 28%, much outpacing the 9% increase in general mortality rates [3]. Cancer death rates vary among regions due to a mix of hereditary and environmental factors. These factors influence the effectiveness of screening campaigns, preventive measures, and treatment options for distinct forms of cancer [4]. The ongoing evolution of medical technologies holds up the possibility of improved screening capabilities as well as, more importantly, advancements in patient care and treatment options. For example, much emphasis has been put into anti-cancer research for developing effective agents, especially compounds that contain benzothiazole and 2-pyridinone moiety [5][6][7][8]. Several studies have been undertaken to improve the anti-cancer activity of benzothiazole by synthesizing a wide range of derivatives. Among these compounds, 2-arylbenzothiazole derivatives have showed promising antitumor activity. For instance, CJM 126, 2-(4-aminophenyl)-benzothiazole **A**, had excellent *in vitro* cytotoxicity in nanomolar concentrations and caused potent growth inhibition against human-derived breast carcinoma cell lines, including oestrogen receptor-positive (ER+) MCF-7wt cells [9]. Additionally, PMX-610, 2-(3,4-dimethoxyphenyl)-5-fluorobenzothiazole **B**, was demonstrated superior *in vivo* efficacy against human breast cancer cell lines MCF-7 and MDA-468 in nanomolar concentrations; however, high lipophilicity restricted its *in vivo* development in aqueous formulations and apparently prevented its development as a chemotherapeutic agent [10]. SAR study of compound **B** revealed that the presence of a methoxy substituent at carbon 3 and 4 of the phenyl ring was important for its antitumor activity; replacing this group with another one resulted in the loss of activity. To overcome this problem, fluorinated analog, 4-(5-fluorobenzothiazol-2-yl)-2-methylaniline **C**, DF 203, has been developed and resolved the metabolic issues [11]. Compound **C**

showed potent antitumor activity against wide spectrum of cancers such as ovarian, breast, collateral, and kidney, Fig. 1 [12].

Over the last two decades, there has been a surge of interest in 2-pyridone derivatives in medicinal development efforts, with numerous FDA-approved medications working as kinase inhibitors. These include recent approvals for Tazemetostat (2020), which stands up as an effective, selective, and orally accessible small-molecule inhibitor of EZH2 [13]. This is crucial because EZH2 inhibitors have promise in cancer treatment, especially in tackling difficulties such as drug resistance, poor distribution, and limited brain penetration reported with several current chemotherapeutic medications, Fig. 2. Additionally, Fredericamycin A is being investigated as a new lead molecule for battling human tumours [14], whilst Camptothecin has been proven to be effective in cancer treatment by blocking DNA topoisomerase I [15], Fig. 2.

.

Several 2-(benzo[*d*]thiazol-2-yl)acetohydrazide derivatives have been developed [16][17] and used for the synthesis of benzothiazole hybrid compounds [18][19][20]. Drawing on our previous successes in developing compounds containing benzothiazole and pyridinone rings, which demonstrated significant antimicrobial [21][22][23] and antiviral activities [24][25][26], we proceeded on a new venture. Building on this foundation, we synthesized new hybrid compounds containing both benzothiazole and pyridinone and tested their potential anticancer properties. Furthermore, we conducted extensive *in-silico* research and docking analysis to better understand the molecular mechanisms behind their interactions and efficacy. This holistic strategy seeks to advance our understanding of these chemicals' therapeutic potential in cancer treatment, establishing the framework for future drug development initiatives.

2. Results and discussions

2.1. Chemistry

Novel *N*-(2-(benzo[*d*]thiazol-2-yl)acetyl)benzohydrazide derivatives **4a-f** were synthesized at first (Scheme 1) and used for the synthesis of new benzothiazole derivatives *N*-(2-(benzo[*d*]thiazol-2-yl)-3-arylacryloyl)benzohydrazide derivatives **7a-g** (Scheme 2), *N*-(6-amino-3-(benzo[*d*]thiazol-2-yl)-2-oxopyridin-1(2*H*)-yl)benzamide derivatives **10a-d** (Scheme 3) and 2-amino-1-benzamido-5-(benzo[*d*]thiazol-2-yl)-6-oxo-*N*-aryl-1,6-dihydropyridine-3-carboxamide derivatives **14a-d** (Scheme 4).

The initial 2-(benzo[*d*]thiazol-2-yl)acetohydrazide **2** was prepared by reacting hydrazine hydrate with ethyl 2-(benzo[*d*]thiazol-2-yl)acetate **1** in ethanol at room temperature for 24 hours [25]. Scheme 1 shows the reaction of benzothiazole hydrazide with benzoyl chloride derivatives **3a-f** in the presence of pyridine at room temperature to produce new starting derivatives of *N*-(2-(benzo[*d*]thiazol-2-yl)acetyl)benzohydrazide **4a-f**. The chloride atoms in benzoyl chloride derivatives were nucleophilically substituted with NH_2 from the hydrazide compound **2**. The structures of these derivatives were validated

using elemental analysis and spectrum data such as IR, ^{1}H NMR, and ^{13}C NMR. The IR spectra of compounds **4a-f** revealed a broad absorption band at 3439 − 3175 cm^{-1}, which corresponded to the NH group. In addition, the IR spectra revealed two distinct lines at 1696 − 1602 cm^{-1}, corresponding to two C = O groups. Moreover, the ^{1}H NMR spectrum of compound **4a** revealed a singlet signal at δ 4.23 ppm, indicating the presence of a CH_2 group. Furthermore, the ^{1}H NMR spectrum of compound **4a** displayed four characteristic signals corresponding to the four protons of benzothiazole ring. These signals are two triplets at δ 7.43 and 7.58 ppm and two doublets at δ 7.98 and 8.06 ppm. In addition, the ^{1}H NMR showed multiplet signal at a range of δ 7.49–7.53 ppm and one doublet signal at δ 7.91 ppm corresponding to the five protons of benzene ring. The ^{13}C NMR spectrum of compound **4a** confirmed the presence of carbon atom of CH_2 group at δ 39.4 ppm and two carbon atoms of C = O groups at δ 165.9 and 167.1 ppm. In order to establish the structure of *N*′-(2-(benzo[*d*]thiazol-2-yl)acetyl)benzohydrazide derivatives **4** unambiguously, the X-ray crystal structure of **4a** was determined, Fig. 3 [17].

Following the preparation of *N*′-(2-(benzo[*d*]thiazol-2-yl)acetyl)benzohydrazide derivatives **4a,d**, the corresponding benzilydine derivatives were synthesized by reacting benzaldehyde derivatives **5a-d** with benzothiazole benzohydrazide compounds **4a,b** using the Knoevenagel condensation reaction. This reaction was carried out in ethanol with a catalytic amount of piperidine at room temperature for 5 hours. The weak base piperidine deprotonated one of the hydrogen atoms in compound **4**'s active methylene group, causing it to attack the carbon of the carbonyl group in benzaldehyde molecule **5**, resulting in intermediate **6**. The latter lost a water molecule, resulting in the formation of *N*′-(2-(benzo[*d*]thiazol-2-yl)-3-phenylacryloyl)benzohydrazide derivatives **7a-g** in good yield (Scheme 2). The structure of compounds **7a-g** were confirmed by their spectroscopic data such as IR, ^{1}H NMR and ^{13}C NMR. The IR spectrum of compound **7b** was characterized by the presence of broad band absorption band at υ 3438 cm^{-1} corresponding to NH group. Additionally, sharp absorption bands appeared at υ 1692 and 1644 cm^{-1} corresponding to two C = O groups. Moreover, the ^{1}H NMR spectrum of the same compound revealed the presence of a singlet signal at δ 7.75 ppm corresponding to the CH proton and two singlet signals at δ 10.74 and δ 10.78 ppm for two NH groups. Furthermore, ^{13}C NMR of **7b** showed two signals appeared at δ 166.2 and 166.4 ppm corresponding to two carbons of two C = O groups.

N′-(2-(benzo[*d*]thiazol-2-yl)acetyl)benzohydrazide derivatives **4a,d** were reacted with ethoxymethylene compounds, 2-(ethoxymethylene)malononitrile **8a** and (*E*)-ethyl 2-cyano-3-ethoxy-acrylate **8b** to synthesize *N*-(6-amino-3-(benzo[*d*]thiazol-2-yl)-5-cyano-2-oxopyridin-1(2*H*)-yl)benzamide **10a,c** and ethyl 2-amino-1-benzamido-5-(benzo[*d*]thiazol-2-yl)-6-oxo-1,6-dihydropyridine-3-carb-oxylate **10b,d**, respectively, Scheme 3. The reaction was carried out in ethanol with one equivalent of potassium hydroxide. This reaction proceeded via Michael addition reaction of the ethoxymethylene compounds with the compounds **4a,d** followed by the elimination of ethanol and intramolecular cyclization through the addition of NH group to the cyano group to afford the *N*-arylcarbamide pyridones **10a-d** products. The elemental analysis and spectral data confirmed the proposed structure of compounds **10a-d**. For

example, IR spectrum of compound **10a** displayed absorption band at υ 3430 cm^{-1} for NH_2 group, as well as a band at υ 2216 cm^{-1} corresponding to the CN group and band at υ 1631 cm^{-1} corresponding to C = O group. Moreover, the ^1H NMR spectrum of **10a-d** was characterized by the presence of singlet signal at δ 8.76 to 8.72 and 9.21 to 9.10 ppm for the CH group of pyridone of **10a,c** and **10b,d**, respectively. Moreover, the presence of protons of the ethyl group was confirmed in the ^1H NMR spectra of compounds **10b,d** by triplet signal at 1.13-1-16 ppm for CH_3 group and quartet signal at 3.96–4.38 ppm for CH_2 group. Additionally, the ^{13}C NMR of compound **10a** revealed signals at δ 118.6, 162.1 and 164.1 ppm corresponding to CN and two C = O groups, respectively.

The target derivatives of 2-amino-1-benzamido-5-(benzo[*d*]thiazol-2-yl)-6-oxo-*N*-phenyl-1,6-dihydropyridine-3-carboxamide derivatives **14a-d** were synthesized starting from the reaction of **4a,d** with *N*-phenyl acrylamide derivatives **13a-c** in basic condition, Scheme 4. The reaction proceeded via Micheal addition and the elimination of $NH(CH_3)_2$ which followed by the intramolecular cyclization resulting from the addition of NH proton to the cyano group to produce **14a-d**. The structure of compounds **14a-d** was established based on spectral data such as IR, ^1H NMR and ^{13}C NMR and elemental analysis. According to the IR spectral analysis of compounds **14a-d**, the appearance of an absorption band at a range of 3489 − 3327 cm^{-1} confirmed the presence of NH group. In addition, the IR spectra showed a sharp band at a range of 1660 − 1623 cm^{-1} which corresponding to C = O group. The ^1H NMR of compound **14c**, as an example, showed three singlet signals which assigned for the protons of CH_3 group, CH group of pyridone and NH group at δ 2.42, 9.23 and 11.68 ppm, respectively. ^1H NMR of compound **14d** displayed four characteristic signals corresponding to the four protons of benzothiazole ring, two triplet signals at δ 7.26 and 7.44 ppm and two doublets at δ 7.92 and 8.02 ppm in addition to four doublet signals for two aryl groups. Additionally, the ^{13}C NMR spectrum of **14c** confirmed the presence of CH_3 carbon δ 21.5 ppm and two C = O carbons at δ 162.5 and 165.0 ppm.

2.2. Biological activity

2.2.1. Anticancer activity.

Compounds **4a-f**, **7a-g**, **10a-d**, **14c** and **14d** were *in vitro* evaluated of their anti-cancer activity against three human cancer cell lines, lung H1299, liver Hepg2 and breast MCF7, using the SRB assay with doxorubicin as the standard drug. Cytotoxicity was evaluated at concentrations of 6.25, 12.5, 25, 50 μg/ml, and the IC_{50} values of the tested compounds were compared to those of the reference drug, as presented in Tables 1, Figs. 4 & 5. Additionally, the surviving fraction was measured and compared with the control group. Anti-cancer activities of the synthesized compounds have showed low activity against lung H1299 cell line. While no compound exhibited higher activities than standard drugs, doxorubicin (DOX), with H1299, benzylidine derivatives **7a-c**, 7e and **7f** showed comparable results with standard drug against Hepg2 and MCF7 cell lines. Additionally, only benzylidine compounds **7a-g** have shown high activities than starting benzoyl derivatives 4a-f as well as other compounds that having benzothiazole bonded with pyrdinone ring **10a-d**, **14c** and **14d** against the three tested cell lines.

Based on IC_{50} values, the synthesized compounds against lung H1299, liver Hepg2 and breast MCF7 cancer cell lines, as shown in Table 1, the structure-activity relationships (SAR) have been established. For instance, both compounds **7a** and **7c** with benzoyl group and either hydrogen atom or methyl group at C4 at the benzene ring, respectively, are showing almost equal activities toward liver Hepg2 and breast MCF7 cell lines (IC_{50} = 5 and 6 µg/ml, respectively). However, introducing chlorine atom to benzene ring, compound **7b**, led to decreasing the activity against the liver Hepg2 cell line and increasing activity against the breast MCF7 cell line (IC_{50} = 11 and 5.5 µg/ml, respectively). On the other hand, the presence of methoxy group at the para position of benzene ring, compound **7d**, led to decreasing the activity against liver Hepg2 and breast MCF7 cell lines (IC_{50} = 32.5 and 43.5 µg/ml, respectively). Alternatively, the presence of 4-methylbenzoyl group and either hydrogen or chlorine atom at C4 of the benzene ring, compounds **7e** and **7f**, resulted in lower activities for these compounds against the breast MCF7 cell line (IC_{50} = 10 and 7.5 µg/ml, respectively) as compared to the corresponding compounds containing non-substituted benzoyl group, **7a** and **7b**. Surprisingly compounds **7e** and **7f**, gave the highest activities against the liver Hepg2 cell line (IC_{50} = 4.5 and 4.48 µg/ml, respectively). Introducing the methoxy group at the para position of benzene ring, compound **7g**, resulted into decreasing the activity against liver Hepg2 and breast MCF7 cell lines (IC_{50} = 16 and 15 µg/ml, respectively). The mentioned data indicated that compounds **7e** and **7f** are the most potent against liver Hepg2 as compared to doxorubicin drug (IC_{50} = 4.73 µg/ml), Fig. 4.

Table 1
Anti-cancer assay of a novel synthesized compounds on Lung cancer cell H1299, Liver cancer Hepg2 and Breast cancer MCF7.

Comp. No.	IC_{50} (µg/ml)		
	H1299	HEPG2	MCF7
DOX	**4.28**	**4.73**	**4.13**
4a	42	24	32
4b	46	40	50+
4c	50+	50+	50+
4d	50+	42	47.8
4e	44	40	50+
4f	50+	35.5	50+
7a	43	5	6
7b	42	11	5.5
7c	41	5.2	6
7d	50+	32.5	43.5
7e	47	4.5	10
7f	50	4.48	7.5
7g	50+	16	15
10a	50+	48.5	42
10b	50	23.5	12
10d	50+	50+	50+
14c	50+	43.5	50+
14d	50+	27	40

2.2.2. *In Silico* ADME Study

Physicochemical, pharmacokinetic/ADME and drug likeness properties

The synthesized compounds' potential as drug candidates was explored through an *in-silico* ADME study using the Swiss ADME online tool. Physicochemical and pharmacokinetic properties of the most potent five compounds, **7a-c**, **7e**, and **7f**, were evaluated and tabulated in Table 2. A molecule's poor oral

bioavailability in drug discovery is often associated with more than five hydrogen bond donors, ten hydrogen bond acceptors, a molecular weight exceeding 500 g/mol, and a calculated Log P above 5. Notably, the molecular weights of all tested compounds are ranging from 399.46 g/mol to 447.94 g/mol which indicates a good bioavailability. These compounds showed moderate numbers of hydrogen bond acceptors and donors, three and two respectively, suggesting potential hydrogen bonding interactions with biological targets. The iLogP values, ranging from 3.1 to 3.6, indicated moderate lipophilicity, essential for drug-like properties. Three compounds, **7a**, **7c** and **7e** showed moderate solubility while two compounds that have chlorine atom, **7b** and **7e**, showed poor solubility. Topological polar surface area (TPSA) of all tested compounds exhibited the same value of 99.33 $Å^2$, which is lower than 140 and indicated good oral bioavailability. Additionally, the predicted high gastrointestinal absorption (GI absorption) of the compounds suggests good potential for oral administration. BOILD-EGG diagram displayed the bioavailability property space for wlog P and TPSA, white area means that intestinal absorption, Fig. 6. All compounds are fail in the white area which suggests these molecules have lower affinity or interaction with P-gp. In the context of bioavailability, Pgp-compounds may have higher absorption rates or lower susceptibility to efflux by P-gp, leading to potentially higher bioavailability. Lack of blood-brain barrier (BBB) penetration of all five potent compounds indicates no central nervous system effects, while non-substrate predictions for P-glycoprotein suggest positive drug absorption and distribution. Moreover, potent benzothiazole derivatives inhibited CYP2C19 and CYP2C9 but not CYP1A2, CYP2D6, or CYP3A4, implying selective CYP inhibition with potential drug-drug interaction relevance. Poor skin permeability is predicted for these compounds due to the negative log Kp values. With adherence to Lipinski, Ghose, Vebe, and Egan's rules for drug-likeness, except for one Muegge violation indicating good oral bioavailability, the compounds exhibited a consistent bioavailability score of 0.55, suggesting moderate potential for oral bioavailability.

Table 2
Physicochemical, Pharmacokinetic/ADME and Drug Likeness properties of compounds **7a-c, 7e** and **7f**

Compounds	**7a**	**7b**	**7c**	**7e**	**7f**
Physicochemical Properties					
Molecular Weight g/mol	399.46	433.91	413.49	413.49	447.94
Rotatable Bonds	7	7	7	7	7
H-bond Acceptors	3	3	3	3	3
H-bond Donors	2	2	2	2	2
iLogP	3.1	3.8	3.43	3.48	3.6
Molar Refractivity	115.32	120.33	120.28	120.28	125.29
Log S	MS	PS	MS	MS	PS
TPSA Å^2	99.33	99.33	99.33	99.33	99.33
Pharmacokinetic/ADME					
GI absorption	High	High	High	High	High
BBB permeability log BB	No	No	No	No	No
P-Gpsubstrate	No	No	No	No	No
CYP1A2 inhibitor	No	No	No	No	No
CYP2C19 inhibitor	Yes	Yes	Yes	Yes	Yes
CYP2C9 inhibitor	Yes	Yes	Yes	Yes	Yes
CYP2D6 inhibitor	No	No	No	No	No
CYP3A4 inhibitor	Yes	Yes	Yes	Yes	Yes
log Kp	-5.24	-5.01	-5.07	-5.07	-4.84
Drug Likeness					
Lipinski violations	0	0	0	0	0
Ghose violations	0	0	0	0	0
Veber violations	0	0	0	0	0
Egan violations	0	0	0	0	0
Muegge violations	0	1	1	1	1
Bioavailability Score	0.55	0.55	0.55	0.55	0.55

Toxicological Properties

The *in silico* predictions of toxicological properties of **7a-c**, **7e** and **7f** compounds were determined using the Osiris property explorer program available online at http://www.propertyexplorer-cheminfo.org and summarized in Table 3. The results showed that all five compounds are predicted to be non-mutagenic and non-tumorigenic. This suggests they are unlikely to cause genetic mutations or cancer. Similarly, none of the compounds are expected to be irritants, indicating they may not cause skin or eye irritation. The compounds are also predicted to have no reproductive effects, meaning they are unlikely to interfere with reproductive health or fetal development. Druglikeness assesses how well a compound resembles known drugs in terms of its physicochemical properties. Scores above zero generally indicate drug-like characteristics. Here, all compounds show positive druglikeness scores, ranging from 2.73 to 5.88. This suggests they possess properties that could make them suitable as drugs. Drug Score evaluates the overall potential of a compound to be developed as a drug, considering various factors like druglikeness and toxicity risks. The drug scores for these compounds range from 0.69 to 0.81. While these values are not exceptionally high, they still indicate some potential for drug development, especially when combined with the absence of predicted mutagenicity, tumorigenicity, and irritant effects.

Table 3
Toxicity prediction of compounds **7a-c, 7e** and **7f**

Compounds	**7a**	**7b**	**7c**	**7e**	**7f**
Mutagenic	No	No	No	No	No
Tumorigenic	No	No	No	No	No
Irritant	No	No	No	No	No
Reproductive effective	No	No	No	No	No
Druglikeness	4.09	5.88	3.75	2.73	4.39
Drug Score	0.81	0.74	0.77	0.76	0.69

2.3. Docking Study

Protein tyrosine kinases (PTKs) are crucial enzymes regulating fundamental cellular processes such as growth, proliferation, and metabolism by transferring phosphate groups from ATP to tyrosine residues on target proteins [27]. Dysregulation of PTKs is associated with various diseases, prominently cancer. In breast cancer, aberrant expression or mutation of PTKs like HER2 and EGFR fuel tumor development, with MCF7 serving as a cornerstone model for studying breast cancer biology and therapeutic responses [28]. Similarly, dysregulated PTKs such as c-Met and FGFR contribute significantly to hepatocellular carcinoma progression, rendering HepG2 invaluable for liver cancer research. These cell lines aid researchers in deciphering the roles of specific PTKs in cancer development, drug responses, and therapeutic targeting, enhancing our understanding of breast and liver cancers at the molecular level. Moreover, to understanding the mechanisms and binding affinity of potent compounds in this study as

anticancer agents **7a-c**, **7e**, and **7f** with specific PTKs, access to docking study results is vital. Integrating these insights provided crucial understanding of compound-PTK interactions, shedding light on their therapeutic potential and guiding future research in this domain. Therefore, docking studies utilizing the crystal structure of the PTK receptor (PDB ID: 2GQG) were undertaken to delineate the interactions of the most promising compounds with the PTK binding site.

The validation process of the docking study involved placing the original ligand (1N1) from the crystal structure into the active site, following its extraction from the respective receptor, as depicted in Fig. 7. Docking of the original ligand 1N1 resulted in a root mean square deviation (RMSD) value of 1.1599 and docking score − 9.2914 kcal/mol. Analysis of the results revealed that 1N1 formed specific interactions within the active site, including one hydrogen bond acceptor with Met318, two hydrogen bond donors with Met318 and Thr315, and one H-arene interaction with Leu248.

The docking study revealed valuable insights into the binding interactions and potential efficacy of compounds **7a-c**, **7e**, and **7f** towards PTK receptor, Table 4 & Fig. 8. Tested compounds exhibited a range of binding affinities, with docking scores varying from − 8.7770 to -8.6343 kcal/mol. This suggests structural differences between these compounds influence their interaction with the target protein. Comparing **7a** and **7b**, as well as **7e** and **7f**, the addition of a chlorine atom seems to slightly increased binding affinity. Additionally, Met318 consistently appears as a crucial interacting residue across all compounds, highlighting its importance in the binding pocket and potential role in the protein's function. They bonded with hydrogen bond acceptors with bond length 2.49 **Å** for **7a-c** and 2.47 **Å** for **7e** and **7f**. While the presence of methyl group on benzoyl ring in compounds **7e** and **7f** clearly contributed to the H-arene interactions with Asp381, it increased the binding affinity as compared with corresponding derivatives **7a** and **7b**. Asp381 participated in interactions with compounds **7e** and **7f**, suggesting that the binding pocket may accommodate diverse ligand structures and utilize different interaction types.

Table 4
Molecular docking score and bond interactions of compounds **7a-c**, **7e** and **7f** with PTK receptor

Comp.	Docking Score (kcal/mol)	rmsd	Types of Interactions	Residues	Bond length Å
7a	-8.7770	1.3945	H-acceptor	Met318	2.49
7b	-8.8507	1.5188	H-acceptor	Met318	2.49
7c	-8.8166	2.1569	H-acceptor	Met318	2.49
7e	-8.6343	1.2071	H-acceptor H-arene	Met318 Asp381	2.47
7f	-8.7165	1.3936	H-acceptor H-arene	Met318 Asp381	2.47

3. Conclusions

In this work, a new class of functionalized benzothiazole bearing benzilidene derivatives or *N*-carboxamide 2-pyridone derivatives were synthesized from a new *N*-aryl carboxohydrazide incorporating benzothiazole moiety, with remarkable anticancer potency. The synthesis was carried out by reacting *N*-aryl carboxohydrazide with benzaldehyde derivatives to produce benzilidene derivatives and with 2-ethoxyl acrylonitrile derivatives or enamine of analide to produce *N*-carboxamide 2-pyridone derivatives. The anticancer activities of the newly synthesized compounds against three cell lines lung H1299, liver HEPG2 and breast cancers MCF7 revealed that five of the newly synthesized compounds showed IC_{50} of anticancer activities with lower than 10 µg/ml against HEPG2 and MCF7 cell lines. Additionally, the IC_{50} of compounds **7e** and **7f** was lower than the IC_{50} of doxorubicin drug. According to the in silico study, potent compounds, **7a-c**, **7e**, and **7f**, as demonstrated promising properties for drug development, including high GI absorption and selective CYP inhibition and exhibited promising characteristics for further investigation as potential drug candidates. Docking studies elucidated binding modes and efficacy of potent compounds as PTK inhibitors. The consistent involvement of Met318 in hydrogen bonding interactions across all compounds underscores its importance in ligand recognition and binding.

4. Experimental section

4.1. Chemistry

All melting points were measured using a SMP3 melting point apparatus. IR spectra were recorded on an FTIR plus 460 or pyeunicam SP-1000 spectrophotometer using KBr pellets. The ^{1}H and ^{13}C NMR spectra were done in the Center of Drug Discovery Research and Development at Ain Shams University, and recorded on a Bruker Avance (III)-400 Spectrometer (400 and 100 MHz, respectively) in DMSO d_6 as a solvent using $Si(CH_3)_4$ as an internal standard and chemical shifts are reported as δ ppm units. Progress of the reactions was monitored by thin-layer chromatography (TLC) using aluminum sheets coated with silica gel F254 (Merck), and UV lamp.

General procedures for preparation compounds (4a-f)

A mixture of 2-(benzo[*d*]thiazol-2-yl)acetohydrazide **2** (0.08 mole) and pyridine (10 mL) were stirred for 15 min. Benzoyl chloride derivatives **3a-f** (0.16 mole) were added gradually to the reaction mixture in ice bath and stirred for 15 min. The reaction mixture was left at room temperature for 3 h. After the completion of the reaction, the solution was poured onto ice water and neutralized with HCl. The solid formed was filtered off and dried to produce a solid product. The solid product formed was washed using suitable solvent.

N '-(2-(Benzo[d]thiazol-2-yl)acetyl)benzohydrazide (4a)

White solid, yield 85%, m.p: 213–214 ^{o}C; IR (KBr, cm^{-1}): υ 3284 (NH), 2974 (CH-Ar), 1696, 1662 (2CO); ^{1}H NMR (400 MHz, DMSO-d_6): δ 4.23 (s, 2H, CH_2), 7.43 (t, J = 7.2 Hz, 1H, benzothiazole-H), 7.49–7.53 (m,

3H, Ar-H), 7.58 (t, *J* = 8.4 Hz, 1H, benzothiazole-H), 7.91 (d, *J* = 7.2 Hz, 2H, Ar-H), 7.99 (d, *J* = 9.6 Hz, 1H, benzothiazole-H), 8.09 (d, *J* = 9.2 Hz, 1H, benzothiazole-H), 10.48 (s, 1H, NH), 10.55 (s, 1H, NH); ^{13}C NMR (100 MHz, DMSO-d_6): δ 39.4 (CH_2), 122.5, 122.8, 125.5, 126.5, 127.9, 128.9, 129.0, 132.4, 132.8, 136.9, 152.7, 165.0 (Ar-C), 165.9, 167.1 (2CO); Anal. calcd for $C_{16}H_{13}N_3O_2S$ (311.36): C% 61.72; H% 4.21; N% 13.50; Found: C% 61.70; H% 4.24; N% 13.55.

N '-(2-(Benzo[d]thiazol-2-yl)acetyl)-4-chlorobenzohydrazide (4b)

White solid, yield 80%, m.p: 225–226 ^{o}C; IR (KBr, cm^{-1}): υ 3264 (NH), 3033 (CH-Ar), 1683, 1655 (2CO); ^{1}H NMR (400 MHz, DMSO-d_6): δ 4.23 (s, 2H, CH_2), 7.44 (t, *J* = 7.8 Hz, 1H, benzothiazole-H), 7.51 (t, *J* = 6.6 Hz, 1H, benzothiazole-H), 7.58 (d, *J* = 10 Hz, 2H, Ar-H), 7.90 (d, *J* = 7.2 Hz, 2H, Ar-H), 7.98 (d, *J* = 8.4 Hz, 1H, benzothiazole-H), 8.09 (d, *J* = 10.8 Hz, 1H, benzothiazole-H), 10.60 (s, 2H, NH); Anal. calcd for $C_{16}H_{12}ClN_3O_2S$ (345.80): C% 55.57; H% 3.50; N% 12.15; Found: C% 55.60; H% 3.48; N% 12.13.

N' -(2-(Benzo[d]thiazol-2-yl)acetyl)-4-bromobenzohydrazide (4c)

White solid, yield 80%, m.p: 238–239 ^{o}C; IR (KBr, cm^{-1}): υ 3265 (NH), 3033 (CH-Ar), 1683, 1656 (2CO); ^{1}H NMR (400 MHz, DMSO-d_6): δ 4.21 (s, 2H, CH_2), 7.44 (t, *J* = 7.2 Hz, 1H, benzothiazole-H), 7.51 (t, *J* = 7.4 Hz, 1H, benzothiazole-H), 7.73 (d, *J* = 8.4 Hz, 2H, Ar-H), 7.83 (d, *J* = 8.4 Hz, 2H, Ar-H), 7.97 (d, *J* = 8 Hz, 1H, benzothiazole-H), 8.09 (d, *J* = 7.2 Hz, 1H, benzothiazole-H), 10.49 (s, 1H, NH), 10.63 (s, 1H, NH); Anal. calcd for $C_{16}H_{12}BrN_3O_2S$ (390.25): C% 49.24; H% 3.10; N% 10.77; Found: C% 49.20; H% 3.13; N% 10.79.

N' -(2-(Benzo[d]thiazol-2-yl)acetyl)-4-methylbenzohydrazide (4d)

White solid, yield 83%, m.p: 193–195 ^{o}C; IR (KBr, cm^{-1}): υ 3190 (NH), 3027 (CH-Ar), 1669, 1602 (2CO); ^{1}H NMR (400MHz, DMSO-d_6): δ 2.36 (s, 3H, CH_3), 4.21 (s, 2H, CH_2), 7.30 (d, *J* = 8.0 Hz, 2H, Ar-H), 7.43 (t, *J* = 6.0 Hz, 1H, benzothiazole-H), 7.51 (t, *J* = 8.0 Hz, 1H, benzothiazole-H), 7.80 (d, *J* = 8.0 Hz, 2H, Ar-H), 7.98 (d, *J* = 8.0 Hz, 1H, benzothiazole-H), 8.08 (d, *J* = 8.0 Hz, 1H, benzothiazole-H), 10.45 (s, 1H, NH), 10.46 (s, 1H, NH); ^{13}C NMR (100MHz, DMSO-d_6): δ 21.4 (CH_3), 39.4 (CH_2), 122.4, 122.7, 125.5, 126.5, 127.9, 129.5, 129.8, 135.7, 142.5, 152.6, 165.0 (13C, Ar-C), 165.9, 167.1 (2CO); Anal. calcd for $C_{17}H_{15}N_3O_2S$ (325.38): C% 62.75; H% 4.65; N% 12.91; Found: C% 62.78; H% 4.67; N% 12.89.

N' -(2-(Benzo[d]thiazol-2-yl)acetyl)-3-methoxybenzohydrazide (4e)

White solid, yield 70%, m.p: 171–172 ^{o}C; IR (KBr, cm^{-1}): υ 3272 (NH), 3027 (CH-Ar), 1693, 1661 (2CO); ^{1}H NMR (400MHz, DMSO-d_6): δ 3.81 (s, 3H, OCH_3), 4.20 (s, 2H, CH_2), 7.40 (d, *J* = 8.8 Hz, 1H, Ar-H), 7.39–7.53 (m, 5H, 3Ar-H & 2benzothiazole-H), 7.98 (d, *J* = 8.8 Hz, 1H, benzothiazole-H), 8.09 (d, *J* = 10.8 Hz, 1H, benzothiazole-H), 10.46 (s, 1H, NH), 10.51 (s, 1H, NH); Anal. calcd for $C_{17}H_{15}N_3O_3S$ (341.38): C% 59.81; H% 4.43; N% 12.31; Found: C% 59.84; H% 4.40; N% 12.34.

N '-(2-(Benzo[d]thiazol-2-yl)acetyl)-2-nitrobenzohydrazide (4f)

Yellowish white solid, yield 68%, m.p: 178–179 ^{o}C; IR (KBr, cm^{-1}): υ 3175 (NH), 3034 (CH-Ar), 1602 (CO); ^{1}H NMR (400MHz, DMSO-d_6): δ 4.21 (s, 2H, CH_2), 7.43 (t, *J* = 8.2 Hz, 1H, benzothiazole-H), 7.51 (t, *J* = 8.8 Hz, 1H, benzothiazole-H), 7.68–8.12 (m, 6H, 4Ar-H & 2benzothiazole-H), 10.75 (s, 1H, NH), 10.79 (s, 1H, NH); Anal. calcd for $C_{16}H_{12}N_4O_4S$ (356.36): C% 53.93; H% 3.39; N% 15.72; Found: C% 53.95; H% 3.35; N% 15.70.

General procedures for preparation compounds (7a-g)

A mixture of *N*-(2-(benzo[*d*]thiazol-2-yl)acetyl)benzohydrazide derivatives **4a,d** (0.01 mole) and benzaldehyde derivatives **5a-d** (0.01 mole) were stirred at room temperature in ethanol containing a catalytic amount of piperidine (3 drops) for 5 h. After the completion of the reaction, the solution was poured onto ice water. The solid formed was filtered, dried, and washed using suitable solvent.

(E)- N '-(2-(Benzo[d]thiazol-2-yl)-3-phenylacryloyl)benzohydrazide (7a)

Yellowish white solid, yield 75%, m.p: 216–217 ^{o}C; IR (KBr, cm^{-1}): υ 3267 (NH), 2993 (CH-Ar), 1641 (CO); ^{1}H NMR (400MHz, DMSO-d_6): δ 7.45–7.58 (m, 7H, 6 Ar-H & 1benzothiazole-H), 7.62 (t, *J* = 6.6 Hz, 1H, benzothiazole-H), 7.75 (s, 1H, CH), 7.97–8.04 (m, 5H, 4Ar-H & 1benzothiazole-H), 8.15 (d, *J* = 8.4 Hz, 1H, benzothiazole-H), 10.73 (s, 1H, NH), 10.89 (s, 1H, NH); Anal. calcd for $C_{23}H_{17}N_3O_2S$ (399.46): C% 69.15; H% 4.29; N% 10.52; Found: C% 69.19; H% 4.28; N% 10.50.

(E)- N '-(2-(Benzo[d]thiazol-2-yl)-3-(4-chlorophenyl)acryloyl)benzohydrazide (7b)

Yellowish white solid, yield 75%, m.p: 232–233 ^{o}C; IR (KBr, cm^{-1}): υ 3268 (NH), 2923 (CH-Ar), 1692, 1644 (2CO); ^{1}H NMR (400MHz, DMSO-d_6): δ 7.47–7.64 (m, 7H, 5Ar-H & 2benzothiazole-H), 7.75 (s, 1H, CH), 7.98–8.03 (m, 5H, 4Ar-H & 1benzothiazole-H), 8.16 (d, *J* = 9.2 Hz, 1H, benzothiazole-H), 10.71 (s, 1H, NH); ^{13}C NMR (400MHz, DMSO-d_6): δ 122.6, 123.2, 126.4, 127.2, 128.1, 128.9, 129.1, 130.9, 132.4, 132.5, 132.8, 132.8, 134.5, 134.8, 134.9, 153.4, 165.5 (Ar-C), 166.2, 166.4 (2CO); Anal. calcd for $C_{23}H_{16}ClN_3O_2S$ (433.91): C% 63.66; H% 3.72; N% 9.68; Found: C% 63.69; H% 3.70; N% 9.72.

(E)- N '-(2-(Benzo[d]thiazol-2-yl)-3-(p -tolyl)acryloyl)benzohydrazide (7c)

Yellowish white solid, yield 73%, m.p: 232–233 ^{o}C; IR (KBr, cm^{-1}): υ 3269 (NH), 2921 (CH-Ar), 1686, 1643 (2CO); ^{1}H NMR (400MHz, DMSO-d_6): δ 2.37 (s, 3H, CH_3), 7.27 (d, *J* = 6.4 Hz, 2H, Ar-H), 7.47 (t, *J* = 7.6 Hz, 1H, benzothiazole-H), 7.53–7.57 (m, 3H, Ar-H), 7.62 (t, *J* = 7.0 Hz, 1H, benzothiazole-H), 7.70 (s, 1H, CH), 7.88 (d, *J* = 7.6 Hz, 2H, Ar-H), 7.99–8.02 (m, 3H, 2Ar-H & benzothiazole-H), 8.14 (d, *J* = 8.0 Hz, 1H, benzothiazole-H), 10.72 (s, 1H, NH), 10.82 (s, 1H, NH); Anal. calcd for $C_{24}H_{19}N_3O_2S$ (413.50): C% 69.71; H% 4.63; N% 10.16; Found: C% 69.74; H% 4.60; N% 10.15.

(E)- N '-(2-(Benzo[d]thiazol-2-yl)-3-(4-methoxyphenyl)acryloyl)benzohydrazide (7d)

Yellow solid, yield 73%, m.p: 215–217 ^{o}C; IR (KBr, cm^{-1}): υ 3270 (NH), 2924 (CH-Ar), 1685, 1645 (CO); ^{1}H NMR (400MHz, DMSO-d_6): δ 3.82 (s, 3H, OCH_3), 7.00 (d, J = 7.6 Hz, 2H, Ar-H), 7.46 (t, J = 8.0 Hz, 1H, benzothiazole-H), 7.52–7.57 (m, 3H, Ar-H), 7.62 (t, J = 7.6 Hz, 1H, benzothiazole-H), 7.67 (s, 1H, CH), 7.95–8.01 (m, 5H, 4Ar-H & 1benzothiazole-H), 8.12 (d, J = 8 Hz, 1H, benzothiazole-H), 10.70 (s, 1H, NH), 10.81 (s, 1H, NH); ^{13}C NMR (400MHz, DMSO-d_6):δ 55.8 (OCH_3), 114.6, 122.5, 122.9, 125.8, 126.4, 127.0, 127.8, 128.2, 128.9, 132.3, 132.9, 133.0, 134.7, 135.8, 153.6, 161.1, 165.9 (Ar-C), 166.3, 166.9 (2CO); Anal. calcd for $C_{24}H_{19}N_3O_3S$ (429.11): C% 67.12; H% 4.46; N% 9.78; Found: C% 67.16; H% 4.49; N% 9.74.

(E)- N' -(2-(Benzo[d]thiazol-2-yl)-3-phenylacryloyl)-4-methylbenzohydrazide (7e)

White solid, yield 65%, m.p: 200–203 ^{o}C; IR (KBr, cm^{-1}): υ 3265 (NH), 2971 (CH-Ar), 1684, 1641 (2CO); ^{1}H NMR (400MHz, DMSO-d_6): δ 2.40 (s, 3H, CH_3), 7.35 (d, J = 8.0 Hz, 2H, Ar-H), 7.44–7.50 (m, 4H, Ar-H & benzothiazole-H), 7.56 (t, J = 7.2 Hz, 1H, benzothiazole-H), 7.74 (s, 1H, CH), 7.90 (d, J = 7.6 Hz, 2H, Ar-H), 7.97–7.99 (m, 2H, Ar-H), 8.02 (d, J = 8.0 Hz, 1H, benzothiazole-H), 8.15 (d, J = 8.4, 1H, benzothiazole-H), 10.71 (s, 2H, NH); Anal. calcd for $C_{24}H_{19}N_3O_2S$ (413.49): C% 69.71; H% 4.63; N% 10.16; Found: C% 69.75; H% 4.65; N% 10.13.

(E)- N '-(2-(Benzo[d]thiazol-2-yl)-3-(4-chlorophenyl)acryloyl)-4-methylbenzohydrazide (7f)

White solid, yield 75%, m.p: 223–224 ^{o}C; IR (KBr, cm^{-1}): υ 3269 (NH), 2923 (CH-Ar), 1686,1645 (CO); ^{1}H NMR (400MHz, DMSO-d_6): δ 2.40 (s, 3H, CH_3), 7.35 (d, J = 8.0 Hz, 2H, Ar-H), 7.47–7.50 (m, 3H, 2Ar-H & 1benzothiazole-H), 7.56 (t, J = 7.8 Hz, 1H, benzothiazole-H), 7.75 (s, 1H, CH), 7.90 (d, J = 8.4 Hz, 2H, Ar-H), 8.00-8.04 (m, 3H, 2Ar-H & 1benzothiazole-H), 8.15 (d, J = 8.4 Hz, 1H, benzothiazole-H), 10.73 (s, 2H, NH); Anal. calcd for $C_{24}H_{18}ClN_3O_2S$ (447.94): C% 64.35; H% 4.05; N% 9.38; Found: C% 64.34; H% 4.06; N% 9.36.

(E)- N' -(2-(Benzo[d]thiazol-2-yl)-3-(4-methoxyphenyl)acryloyl)-4-methylbenzohydrazide (7g)

Off white solid, yield 75%, m.p: 241–243 ^{o}C; IR (KBr, cm^{-1}): υ 3278 (NH), 2953 (CH-Ar), 1681, 1636 (2CO); ^{1}H NMR (400MHz, DMSO-d_6): δ 2.39 (s, 3H, CH_3), 3.86 (s, 3H, OCH_3), 6.99 (d, J = 9.2 Hz, 2H, Ar-H), 7.35 (d, J = 13.6 Hz, 2H, Ar-H), 7.45 (t, J = 11.6 Hz, 1H, benzothiazole-H), 7.54 (t, J = 9.8 Hz, 1H, benzothiazole-H), 7.69 (s, 1H, CH), 7.93 (d, J = 11.6 Hz, 2H, Ar-H), 7.97–8.02 (m, 3H, 2Ar-H & benzothiazole-H), 8.12 (d, J = 9.0 Hz, 1H, benzothiazole-H), 10.64 (s, 1H, NH), 10.77 (s, 1H, NH); Anal. calcd for $C_{25}H_{21}N_3O_3S$ (443.52): C% 67.70; H% 4.77; N% 9.47; Found: C% 67.73; H% 4.75; N% 9.44.

General procedures for preparation of compounds (10a-d)

A mixture of *N'*-(2-(benzo[*d*]thiazol-2-yl)acetyl)benzohydrazide derivatives **4a,d** (0.01 mole) and 2-(ethoxymethylene)malononitrile **8a** or (*E*)-ethyl 2-cyano-3-ethoxyacrylate **8b** (0.017 mole) were refluxed in ethanol (30 ml) containing sodium ethoxide (0.01 mole) for 5 hours. The formed precipitate was filtered then washed using suitable solvent after drying.

N -(6-Amino-3-(benzo[d]thiazol-2-yl)-5-cyano-2-oxopyridin-1(2 H)-yl)benzamide (10a)

Orange solid, yield 70%, m.p: over 350 ^{o}C; IR (KBr, cm^{-1}): υ 3430 (NH, NH_2), 2924 (CH-Ar), 2216 (CN), 1631 (CO); ^{1}H NMR (400MHz, DMSO-d_6): δ 7.30 (t, J = 9.8 Hz, 1H, benzothiazole-H), 7.45–7.56 (m, 4H, 3Ar-H & 1benzothiazole-H), 7.89 (d, J = 9.2 Hz, 1H, benzothiazole-H), 8.04 (d, J = 9.6 Hz, 1H, benzothiazole-H), 8.23 (d, J = 6.0 Hz, 2H, Ar-H), 8.73 (s, 1H, pyridone-H); ^{13}C NMR (400MHz, DMSO-d_6): δ 118.6 (CN), 76.7, 103.9, 121.2, 122.0, 123.6, 126.1, 127.2, 129.2, 130.2, 131.4, 135.0, 136.8, 152.4, 153.7, 156.4 (Ar-C), 162.1, 164.1 (2CO); Anal. calcd for $C_{20}H_{13}N_5O_2S$ (387.41): C% 62.00; H% 3.38; N% 18.08; Found: C% 62.02; H% 3.40; N% 18.06.

Ethyl 2-amino-1-benzamido-5-(benzo[d]thiazol-2-yl)-6-oxo-1,6-dihydropyridine-3-carboxylate (10b)

Orange solid, yield 65%, m.p: over 350 ^{o}C; IR (KBr, cm^{-1}): υ 3433 (NH, NH_2), 2925 (CH-Ar), 1685, 1614 (2CO); ^{1}H NMR (400MHz, DMSO-d_6): δ 1.16 (t, J = 9.0 Hz, 3H, CH_3), 3.97 (q, J = 7.6 Hz, 2H, CH_2), 7.25 (t, J = 8.8 Hz, 1H, benzothiazole-H), 7.41 (t, J = 9.2 Hz, 1H, benzothiazole-H), 7.45–7.54 (m, 3H, Ar-H), 7.87 (d, J = 8.8 Hz, 1H, benzothiazole-H), 7.98 (d, J = 9.2 Hz, 1H, benzothiazole-H), 8.22 (d, J = 9.2 Hz, 2H, Ar-H), 9.10 (s, 1H, pyridone-H); Anal. calcd for $C_{22}H_{18}N_4O_4S$ (434.47): C% 60.82; H% 4.18; N% 12.90; Found: C% 60.83; H% 4.20; N% 12.91.

N -(6-Amino-3-(benzo[d]thiazol-2-yl)-5-cyano-2-oxopyridin-1(2 H)-yl)-4-methylbenzamide (10c)

Orange solid, yield 70%, m.p: over 350 ^{o}C; IR (KBr, cm^{-1}): υ 3423 (NH, NH_2), 3057 (CH-Ar), 2223 (CN), 1643 (2CO); ^{1}H NMR (400MHz, DMSO-d_6): δ 2.43 (s, 3H, CH_3), 7.34 (t, J = 8.8 Hz, 1H, benzothiazole-H), 7.40 (d, J = 7.6 Hz, 2H, Ar-H), 7.48 (t, J = 7.8 Hz, 1H, benzothiazole-H), 7.92–7.97 (m, 3H, 2Ar-H & 1benzothiazole-H), 8.04 (d, J = 8.0 Hz, 1H, benzothiazole-H), 8.67 (s, 1H, pyridone-H), 8.71 (s, 2H, NH_2), 11.27 (s, 1H, NH); Anal.calcd for $C_{21}H_{15}N_5O_2S$ (401.44): C% 62.83; H% 3.77; N% 17.45; Found: C% 62.85; H% 3.79; N% 17.42.

Ethyl 2-amino-5-(benzo[d]thiazol-2-yl)-1-(4-methylbenzamido)-6-oxo-1,6-dihydropyridine-3-carboxylate (10d)

Orange solid, yield 65%, m.p: over 350 ^{o}C; IR (KBr, cm^{-1}): υ 3433 (NH, NH_2), 2920 (CH-Ar), 1685, 1614 (2CO); ^{1}H NMR (400MHz, DMSO-d_6): δ 1.39 (t, J = 7.4 Hz, 3H, CH_3), 2.44 (s, 3H, CH_3), 4.38 (q, J = 7.0 Hz, 2H, CH_2), 7.34 (t, J = 8.8 Hz, 1H, benzothiazole-H), 7.42 (d, J = 12.0 Hz, 2H, Ar-H), 7.48 (t, J = 8.8 Hz, 1H, benzothiazole-H), 7.95-8.00 (m, 3H, 2Ar-H & 1benzothiazole-H), 8.04 (d, J = 8.0 Hz, 1H, benzothiazole-H), 8.86 (s, 2H, NH_2), 9.12 (s, 1H, pyridone-H), 11.05 (s, 1H, NH); Anal. calcd for $C_{23}H_{20}N_4O_4S$ (448.49): C% 61.59; H% 4.49; N% 12.49; Found: C% 61.61; H% 4.47; N% 12.47.

General procedures for preparation of compounds (14a-d)

A mixture of *N*-(2-(benzo[*d*]thiazol-2-yl)acetyl)benzohydrazide derivatives **4a,d** (0.01 mole) and (*Z*)-2-cyano-3-(dimethylamino)-*N*-arylacrylamide derivatives **13a-c** (0.01 mole) were refluxed in dioxane containing equimolar of KOH (0.01 mole) for 7 hours. The precipitate formed was filtered then after drying it was washed using a suitable solvent.

2-Amino-1-benzamido-5-(benzo[]thiazol-2-yl)-6-oxo–phenyl-1,6-dihydropyridine-3-carboxamide (14a)

2-Amino-1-benzamido-5-(benzo[*d*]thiazol-2-yl)-6-oxo-*N*-phenyl-1,6-dihydropyridine-3-carboxamide (14a)
Offwhite solid, yield 65%, m.p: over 350 ^{o}C; IR (KBr, cm^{-1}): υ 3430, 3328 (NH, NH_2), 2938 (CH-Ar), 1631 (CO); ^{1}H NMR (400MHz, DMSO-d_6): δ 7.12–7.28 (m, 2H, benzothiazole-H), 7.44-7-61 (m, 6H, Ar-H), 7.87–7.94 (m, 3H, 2Ar-H & benzothiazole-H), 8.03 (d, J = 8.4 Hz, 1H, benzothiazole-H), 8.30–3.32 (m, 2H, Ar-H), 9.25 (s, 1H, pyridone-H), 11.61 (s, 1H, NH); Anal. calcd for $C_{26}H_{19}N_5O_3S$ (481.53): C% 64.85; H% 3.98; N% 14.54; Found: C% 64.87; H% 3.97; N% 14.53.

2-Amino-1-benzamido-5-(benzo[]thiazol-2-yl)–(4-chlorophenyl)-6-oxo-1,6-dihydropyridine-3-carboxamide (14b)

2-Amino-1-benzamido-5-(benzo[*d*]thiazol-2-yl)-*N*-(4-chlorophenyl)-6-oxo-1,6-dihydropyridine-3-carboxamide (14b)
Beige solid, yield 75%, m.p: over 350 ^{o}C; IR (KBr, cm^{-1}): υ 3435, 3327 (NH, NH_2), 2936 (CH-Ar), 1624 (CO); ^{1}H NMR (400MHz, DMSO-d_6): δ 7.24–7.31 (m, 3H, 2Ar-H & benzothiazole-H), 7.40–7.49 (m, 4H, 3Ar-H & 1benzothiazole-H), 7.53 (d, *J* = 8.4 Hz, 2H, Ar-H), 7.89–7.93 (m, 3H, 2Ar-H & benzothiazole-H), 8.03 (d, *J* = 6.4 Hz, 1H, benzothiazole-H), 9.25 (s, 1H, pyridone-H), 11.45 (s, 2H, NH), 11.66 (s, 2H, NH); Anal. calcd for $C_{26}H_{18}ClN_5O_3S$ (515.97): C% 60.52; H% 3.52; N% 13.57; Found: C% 60.53; H% 3.54; N% 13.56.

2-Amino-5-(benzo[]thiazol-2-yl)–(4-chlorophenyl)-1-(4-methylbenzamido)-6-oxo-1,6-dihydropyridine-3-carboxamide (14c)

2-Amino-5-(benzo[*d*]thiazol-2-yl)-*N*-(4-chlorophenyl)-1-(4-methylbenzamido)-6-oxo-1,6-dihydropyridine-3-carboxamide (14c)
Offwhite solid, yield 73%, m.p: over 350 ^{o}C; IR (KBr, cm^{-1}): υ 3489, 3224 (NH, NH_2), 2916 (CH-Ar), 1660, 1614 (2CO); ^{1}H NMR (400MHz, DMSO-d_6): δ 2.42 (s, 3H, CH_3), 7.30 (t, *J* = 11.0 Hz, 1H, benzothiazole-H), 7.40–7.49 (m, 5H, 4Ar-H & 1benzothiazole-H), 7.89–7.94 (m, 3H, 2Ar-H & 1benzothiazole-H), 8.01 (d, *J* = 9.6 Hz, 1H, benzothiazole-H), 8.20 (d, *J* = 10.0 Hz, 2H, Ar-H), 9.23 (s, 1H, pyridone-H), 11.68 (s, 1H, NH)); ^{13}C NMR (400MHz, DMSO-d_6): δ 21.5 (CH_3), 98.9, 103.9, 121.1, 121.9, 123.3, 125.9, 126.8, 127.2, 128.4, 129.4, 129.9, 134.4, 135.2, 138.9, 139.9, 152.7, 156.6, 160.7 (Ar-C), 162.5, 165.0 (2CO); Anal. calcd for $C_{27}H_{20}ClN_5O_3S$ (530.00): C% 61.19; H% 3.80; N% 13.21; Found: C% 61.22; H% 3.84; N% 13.20.

2-Amino-5-(benzo[]thiazol-2-yl)-1-(4-methylbenzamido)-6-oxo–(-tolyl)-1,6-dihydropyridine-3-carboxamide (14d)

2-Amino-5-(benzo[*d*]thiazol-2-yl)-1-(4-methylbenzamido)-6-oxo-*N*-(*p*-tolyl)-1,6-dihydropyridine-3-carboxamide (14d)

Beige solid, yield 62%, m.p: over 350 ^{o}C; IR (KBr, cm^{-1}): υ 3500, 3330 (NH, NH_2), 2915 (CH-Ar), 1624, 1610 (2CO); ^{1}H NMR (400MHz, DMSO-d_6): δ 2.32 (s, 3H, CH_3), 2.42 (s, 3H, CH_3), 7.23 (d, *J* = 8.4 Hz, 2H, Ar-H), 7.29 (t, *J* = 7.2 Hz, 1H, benzothiazole-H), 7.40–7.46 (m, 3H, 2Ar-H & benzothiazole-H), 7.74 (d, *J* = 9.2 Hz, 2H, Ar-H), 7.92 (d, *J* = 7.6 Hz, 1H, benzothiazole-H), 8.02 (d, *J* = 6.0 Hz, 1H, benzothiazole-H), 8.19 (d, *J* = 8.0 Hz, 2H, Ar-H), 9.23 (s, 1H, pyridone-H), 11.54 (s, 1H, NH); Anal. calcd for $C_{28}H_{23}N_5O_3S$ (509.15): C% 66.00; H% 4.55; N% 13.74; Found: C% 66.02; H% 4.53; N% 13.72.

4.2. Anticancer activity

Human tumor carcinoma cell lines (H1299- HEPG2- MCF7) were used in this study were obtained from the American Type Culture Collection (ATCC, Minisota, U.S.A.). The tumor cell lines were maintained at the National Cancer Institute, Cairo, Egypt, by serial sub-culturing. Samples were prepared by dissolving 1:1 Stock solution and stored at -20˚C in DMSO at 100 mM. Different concentrations of the drug were used 0.00, 6.25, 12.5, 25, 50 µg/ml.

The cytotoxicity was carried out using SRB (used as a protein dye) assay [29]. Cells were seeded in 96-well microtiter plates at initial concentration of 3x10^3 cell/well in a 150 µl fresh medium and left for 24 h for attachment. Different concentrations 0, 6.25, 12.5, 25, 50 µg/ml of drug were added in triplicate for each drug concentration. The plates were incubated for 48 h at 37°C, 5% CO_2. By the end of incubation, cells were fixed with 50 µl cold trichloroacetic acid 10% final concentration for 1 h at 4°C. The plates were washed with distilled water using (automatic washer Tecan, Germany) and stained with 50 µl 0.4% SRB dissolved in 1% acetic acid for 30 minutes at room temperature. The plates were washed four times with 1% acetic acid and air-dried, followed by addition of 200 ml 10 mM Tris base solution (pH 10.5) to each well and shake the plate on a gyratory shaker for 5 min to solubilize the protein-bound dye. Optical density (O.D.) of each well was measured spectrophoto metrically at 570 nm with an ELISA microplate reader (Sunrise Tecan reader, Germany). The mean background absorbance was automatically subtracted and mean values of each drug concentration was calculated. The experiment was repeated 3 times. The percentage of cell survival was calculated after subtraction of background blank O.D. as follows:

Surviving fraction = O.D. (treated cells)/ O.D. (untreated cells).

The IC_{50} values (the concentrations of drug required to produce 50% inhibition of cell growth) were also calculated using GraphPad Prism 8.

4.3. *In Silico* ADME Study

Drug-likeness is a qualitative notion in drug design that predicts a drug-like feature. therapeutic-like qualities such as solubility, permeability, transporter effects, and metabolic stability are essential for therapeutic candidates' success. They have an influence on oral bioavailability, toxicity, metabolism, clearance, and in vitro pharmacology. The drug-likeness of the synthesized compounds was evaluated using five independent filters, including the Lipinski [28], Ghose [30], Muegge [31], Veber [32], and Egan [33] guidelines, as well as bioavailability and drug-likeness scores using the Swiss ADME program.

4.4. Molecular Docking Study

The molecular experiments were conducted using the Molecular Operating Environment (MOE 2014). The ligand molecules were pulled by the building molecule, and their energy was reduced. All minimizations were performed until the MMFF94X force field achieved an rmsd gradient of 0.01 kcal/mol, at which point the partial charges were calculated automatically. Docking simulations were carried out utilizing the Protein Data Bank's crystal structure of the PTK receptor in association with 1N1 (PDB ID: 2GQG). The MOE protonate 3D application was used to add the missing hydrogens and assign the right ionization states. The MOE-Alpha site finder was used to create the active site. The obtained alpha spheres were utilized to make dummy atoms. Ligands were then docked within the active sites using the MOE-Dock. The GBVI/WSA DG free-energy estimates were used to rank the optimized poses and docking poses were examined visually. The interactions with binding pocket residues were finally investigated.

Declarations

Author contributions

Conceptualization: GHE, RAA; Methodology: GHE, RAA, MMS, MAE; Writing-original draft preparation: GHE, RAA; Writing-review and editing: GHE, RAA and MAE.

Funding

Open access funding provided by The Science, Technology & Innovation Funding Authority (STDF) in cooperation with The Egyptian Knowledge Bank (EKB).

Availability of data and materials

The datasets generated during and/or analyzed during the current study are available from the corresponding author.

Ethics approval and consent to participate

Not applicable.

Consent for publication

Not applicable.

Competing interests

The authors declare no competing interests

References

1. Lin H-Y, Park JY. Epidemiology of Cancer. in Anesthesia for Oncological Surgery. Cham: Springer International Publishing; 2023. pp. 11–6.
2. Ferlay J et al. Aug., Cancer statistics for the year 2020: An overview, *Int. J. Cancer*, vol. 149, no. 4, pp. 778–789, 2021, 10.1002/ijc.33588.
3. Allemani C et al. Mar., Global surveillance of cancer survival 1995–2009: analysis of individual data for 25 676 887 patients from 279 population-based registries in 67 countries (CONCORD-2), *Lancet*, vol. 385, no. 9972, pp. 977–1010, 2015, 10.1016/S0140-6736(14)62038-9.
4. Morgan E, et al. Global burden of colorectal cancer in 2020 and 2040: incidence and mortality estimates from GLOBOCAN. Gut. Feb. 2023;72(2):338–44. 10.1136/gutjnl-2022-327736.
5. Lin S, et al. Recent Advances of Pyridinone in Medicinal Chemistry. Front Chem. Mar. 2022;10. 10.3389/fchem.2022.869860.
6. Alrooqi M et al. Sep., A Therapeutic Journey of Pyridine-based Heterocyclic Compounds as Potent Anticancer Agents: A Review (From 2017 to 2021), *Anticancer. Agents Med. Chem.*, vol. 22, no. 15, pp. 2775–2787, 2022, 10.2174/1871520622666220324102849.
7. Kamal A, Syed MAH, Mohammed SM. Therapeutic potential of benzothiazoles: A patent review (2010–2014). Expert Opin Ther Pat. 2015;25(3):335–49. 10.1517/13543776.2014.999764.
8. Pathak N, Rathi E, Kumar N, Kini SG, Rao CM. A Review on Anticancer Potentials of Benzothiazole Derivatives. Mini-Reviews Med Chem. Jan. 2020;20(1):12–23. 10.2174/1389557519666190617153213.
9. Bradshaw T, Wrigley S, Shi D-F, Schultz R, Paull K, Stevens M. 2-(4-Aminophenyl)benzothiazoles: novel agents with selective profiles of in vitro anti-tumour activity, *Br. J. Cancer*, vol. 77, no. 5, pp. 745–752, Mar. 1998, 10.1038/bjc.1998.122.
10. Tan BS et al. Oct., CYP2S1 and CYP2W1 Mediate 2-(3,4-Dimethoxyphenyl)-5-Fluorobenzothiazole (GW-610, NSC 721648) Sensitivity in Breast and Colorectal Cancer Cells, *Mol. Cancer Ther.*, vol. 10, no. 10, pp. 1982–1992, 2011, 10.1158/1535-7163.MCT-11-0391.
11. Bradshaw T, Stevens MF, Westwell A. The Discovery of the Potent and Selective Antitumour Agent 2-(4-Amino-3-methylphenyl)benzothiazole (DF 203) and Related Compounds, *Curr. Med. Chem.*, vol. 8, no. 2, pp. 203–210, Feb. 2001, 10.2174/0929867013373714.
12. Keri RS, Patil MR, Patil SA, Budagumpi S. A comprehensive review in current developments of benzothiazole-based molecules in medicinal chemistry. Eur J Med Chem. Jan. 2015;89:207–51. 10.1016/j.ejmech.2014.10.059.

13. Zhang Y, Pike A. Pyridones in drug discovery: Recent advances. Bioorg Med Chem Lett. Apr. 2021;38:127849. 10.1016/j.bmcl.2021.127849.
14. PANDEY RC, et al. Fredericamycin A a new antitumor antibiotic. I. Production, isolation and physicochemical properties. J Antibiot (Tokyo). 1981;34(11):1389–401. 10.7164/antibiotics.34.1389.
15. Venditto VJ, Simanek EE. Cancer Therapies Utilizing the Camptothecins: A Review of the in Vivo Literature, *Mol. Pharm.*, vol. 7, no. 2, pp. 307–349, Apr. 2010, 10.1021/mp900243b.
16. Azzam RA, Elgemeie GH, Elsayed RE, Jones PG. Crystal structure of N '-[2-(benzo[d]thiazol-2-yl)acetyl]-4-methylbenzenesulfonohydrazide. Acta Crystallogr Sect E Crystallogr Commun. 2017;73:1041–3. 10.1107/S2056989017008738.
17. Azzam RA, Elgemeie GH, Seif MM, Jones PG. Crystal structure of N '-[2-(benzo[d]thiazol-2-yl)acetyl]benzohydrazide, an achiral compound crystallizing in space group P 1 with Z = 1, *Acta Crystallogr. Sect. E Crystallogr. Commun.*, vol. 77, no. 9, pp. 891–894, Sep. 2021, 10.1107/S2056989021007672.
18. Khedr MA, Zaghary WA, Elsherif GE, Azzam RA, Elgemeie GH. Purine analogs: synthesis, evaluation and molecular dynamics of pyrazolopyrimidines based benzothiazole as anticancer and antimicrobial CDK inhibitors, *Nucleosides. Nucleotides Nucleic Acids*, vol. 42, no. 1, pp. 77–104, Jan. 2023, 10.1080/15257770.2022.2109169.
19. Azzam RA, Elgemeie GH, Osman RR, Jones PG. Crystal structure of potassium [4-amino-5-(benzo-[d]thiazol-2-yl)-6-(methylsulfanyl)pyrimidin-2-yl]-(phenylsulfonyl)azanide dimethylformamide monosolvate hemihydrate. Acta Crystallogr Sect E Crystallogr Commun. 2019;75:367–71. 10.1107/S2056989019002275.
20. Elboshi HA, Azzam RA, Elgemeie GH, Jones PG. Crystal structure of 4-(benzo[d]thiazol-2-yl)-1,2-dimethyl-1 H -pyrazol-3(2 H)-one, *Acta Crystallogr. Sect. E Crystallogr. Commun.*, vol. 80, no. 3, pp. 289–291, Mar. 2024, 10.1107/S2056989024001257.
21. Azzam RA, Elsayed RE, Elgemeie GH. Design, Synthesis, and Antimicrobial Evaluation of a New Series of N-Sulfonamide 2-Pyridones as Dual Inhibitors of DHPS and DHFR Enzymes. ACS Omega. 2020;5(18):10401–14. 10.1021/acsomega.0c00280.
22. Azzam RA, Elboshi HA, Elgemeie GH. Synthesis, Physicochemical Properties and Molecular Docking of New Benzothiazole Derivatives as Antimicrobial Agents Targeting DHPS Enzyme. Antibiotics. Dec. 2022;11(12):1799. 10.3390/antibiotics11121799.
23. Elsayed RE, Madkour TM, Azzam RA. Tailored-design of electrospun nanofiber cellulose acetate/poly(lactic acid) dressing mats loaded with a newly synthesized sulfonamide analog exhibiting superior wound healing. Int J Biol Macromol. 2020;164:1984–99. 10.1016/j.ijbiomac.2020.07.316.
24. Azzam RA, Elboshi HA, Elgemeie GH. Novel Synthesis and Antiviral Evaluation of New Benzothiazole-Bearing N -Sulfonamide 2-Pyridone Derivatives as USP7 Enzyme Inhibitors, *ACS Omega*, vol. 5, no. 46, pp. 30023–30036, Nov. 2020, 10.1021/acsomega.0c04424.

25. Azzam RA, Elsayed RE, Elgemeie GH. Design and Synthesis of a New Class of Pyridine-Based N-Sulfonamides Exhibiting Antiviral, Antimicrobial, and Enzyme Inhibition Characteristics. ACS Omega. 2020;5(40):26182–94. 10.1021/acsomega.0c03773.
26. Azzam RA, Elgemeie GH, Osman RR. Synthesis of novel pyrido[2,1-b]benzothiazole and N-substituted 2-pyridylbenzothiazole derivatives showing remarkable fluorescence and biological activities. J Mol Struct. 2020;1201. 10.1016/j.molstruc.2019.127194.
27. Hubbard SR, Till JH. Protein Tyrosine Kinase Structure and Function, *Annu. Rev. Biochem.*, vol. 69, no. 1, pp. 373–398, Jun. 2000, 10.1146/annurev.biochem.69.1.373.
28. Huang G, Cierpicki T, Grembecka J. 2-Aminobenzothiazoles in anticancer drug design and discovery. Bioorg Chem. 2023;135:106477. 10.1016/j.bioorg.2023.106477.
29. Vichai V, Kirtikara K. Sulforhodamine B colorimetric assay for cytotoxicity screening, *Nat. Protoc.*, vol. 1, no. 3, pp. 1112–1116, Aug. 2006, 10.1038/nprot.2006.179.
30. Ghose AK, Viswanadhan VN, Wendoloski JJ. A Knowledge-Based Approach in Designing Combinatorial or Medicinal Chemistry Libraries for Drug Discovery. 1. A Qualitative and Quantitative Characterization of Known Drug Databases, *J. Comb. Chem.*, vol. 1, no. 1, pp. 55–68, Jan. 1999, 10.1021/cc9800071.
31. Muegge I, Heald SL, Brittelli D. Simple Selection Criteria for Drug-like Chemical Matter, *J. Med. Chem.*, vol. 44, no. 12, pp. 1841–1846, Jun. 2001, 10.1021/jm015507e.
32. Veber DF, Johnson SR, Cheng H-Y, Smith BR, Ward KW, Kopple KD. Molecular Properties That Influence the Oral Bioavailability of Drug Candidates, *J. Med. Chem.*, vol. 45, no. 12, pp. 2615–2623, Jun. 2002, 10.1021/jm020017n.
33. Lagorce D, Sperandio O, Galons H, Miteva MA, Villoutreix BO. FAF-Drugs2: Free ADME/tox filtering tool to assist drug discovery and chemical biology projects, *BMC Bioinformatics*, vol. 9, no. 1, p. 396, Dec. 2008, 10.1186/1471-2105-9-396.

Schemes

Schemes 1 to 4 are available in the Supplementary Files section

Figures

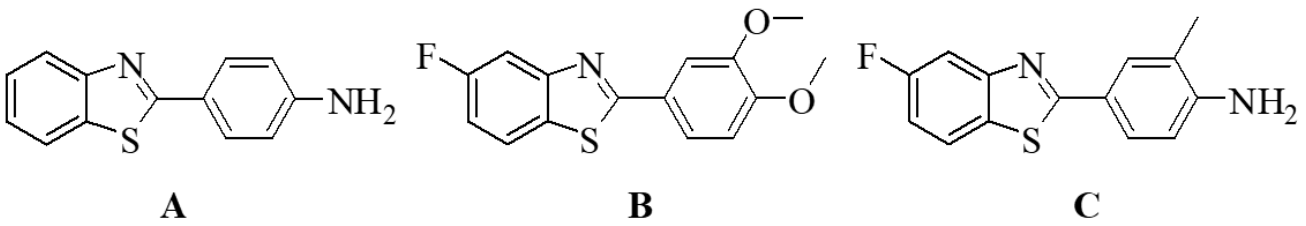

Figure 1

Examples of potent anticancer benzothiazole derivatives

.

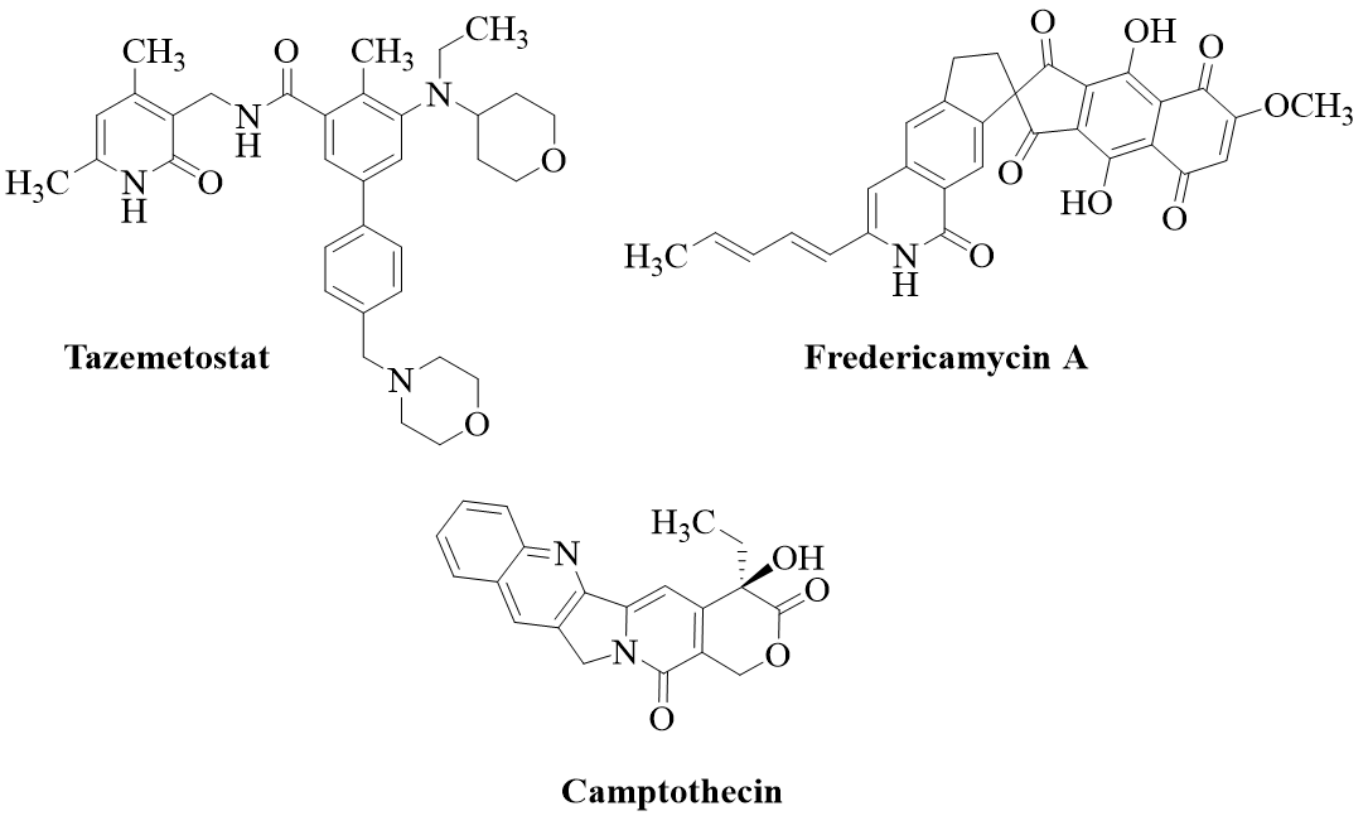

Figure 2

Anticancer drugs containing 2-pyrdinone

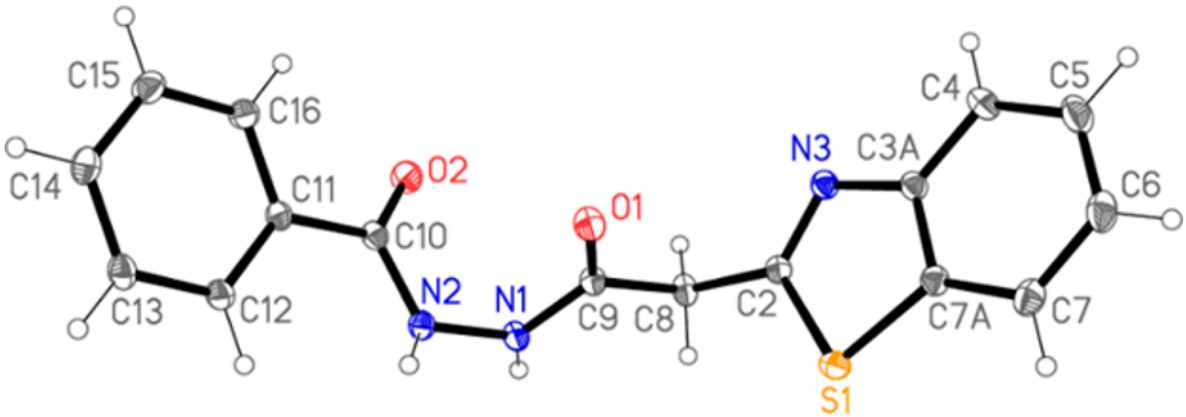

Figure 3

The structure of compound **4a** in the crystal [17].

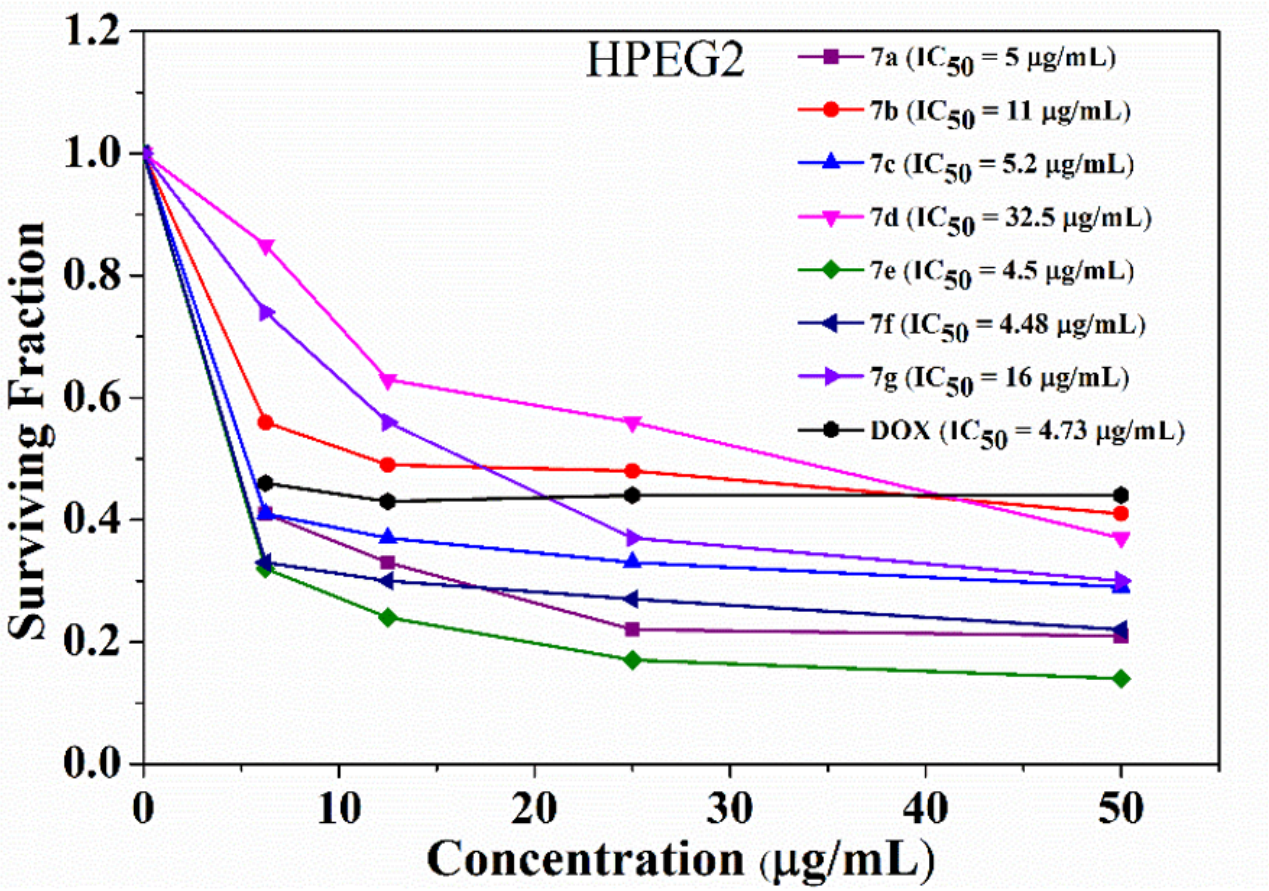

Figure 4

Surviving fraction using SRB on Hpeg2 cell line with compounds **7a-g** and DOX

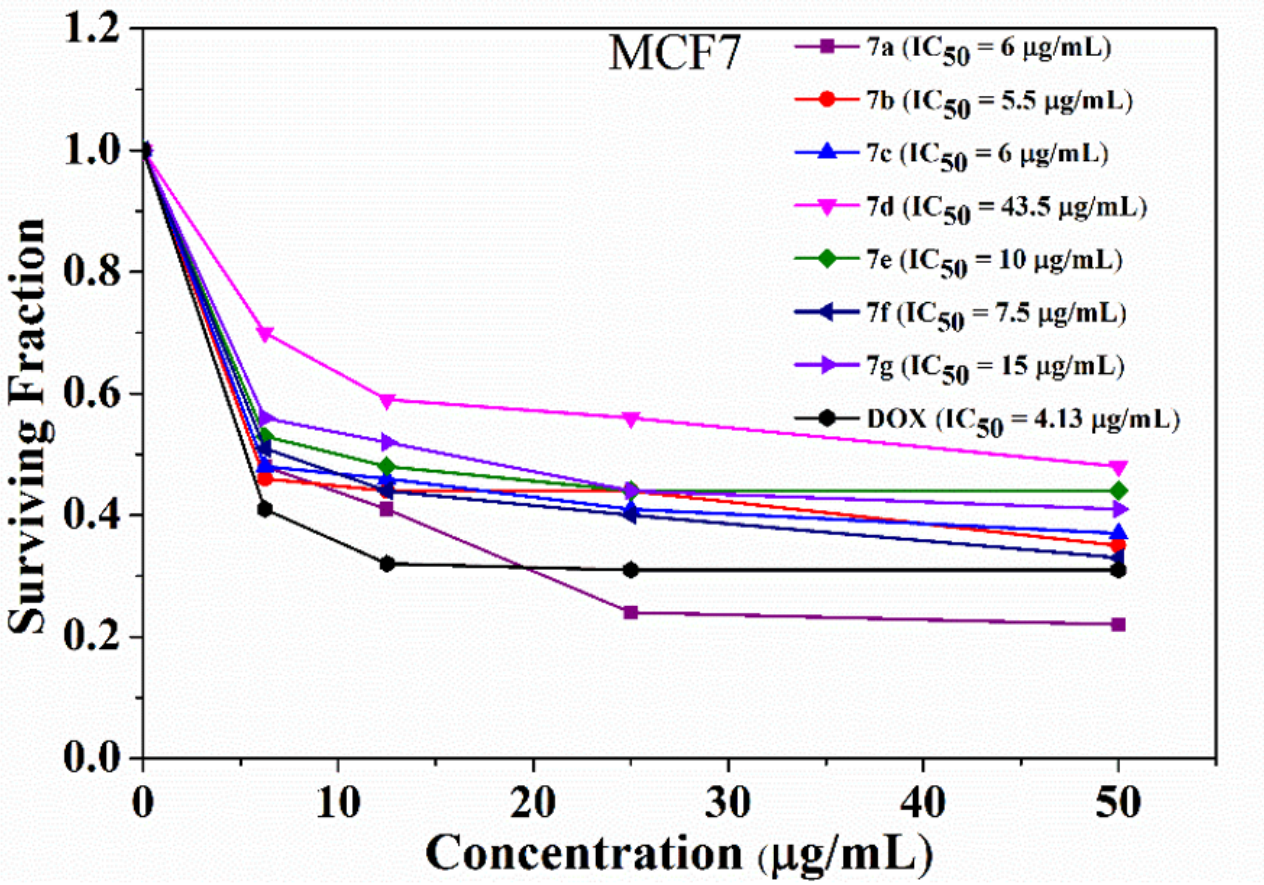

Figure 5

Surviving fraction using SRB on MCF7 cell line with compounds **7a-g** and DOX

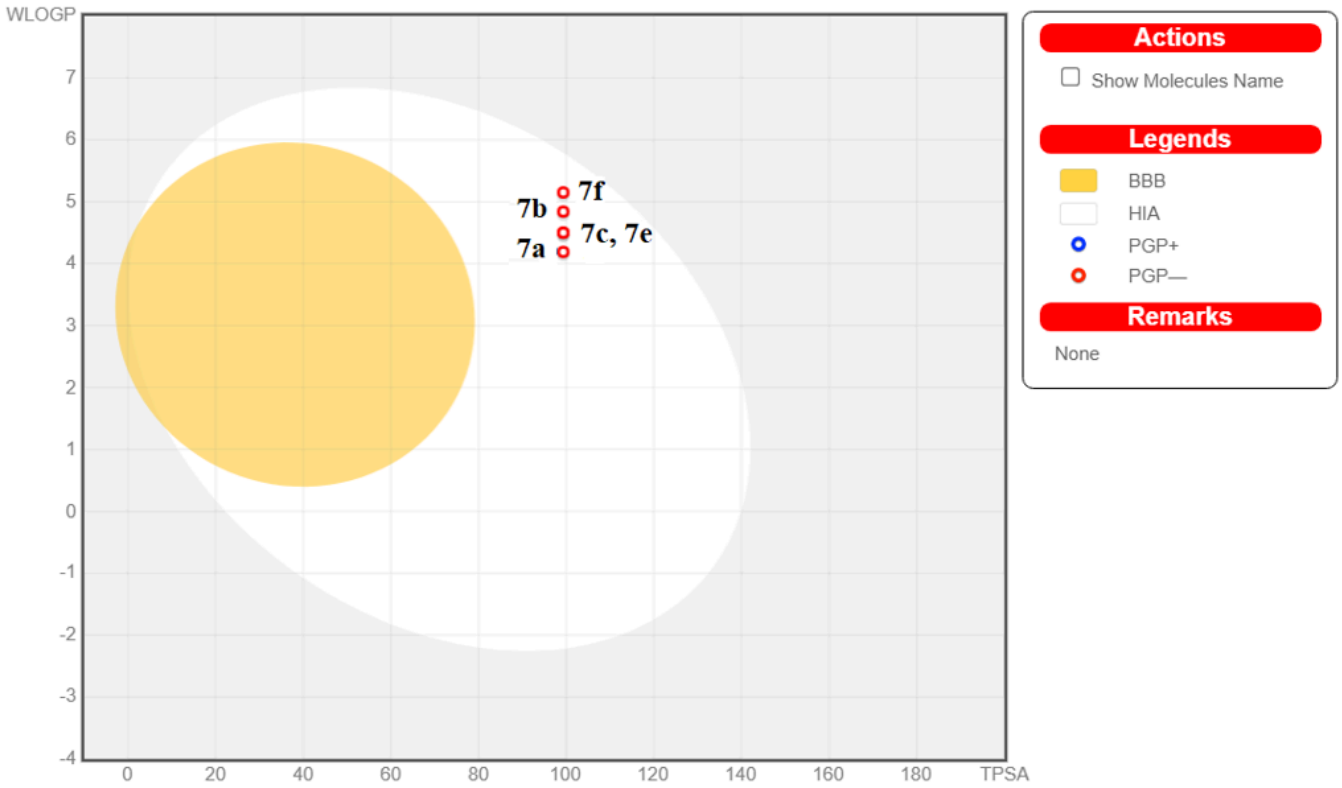

Figure 6

DOILED-EGG diagram of tested compounds **7a-c**, **7e** and **7f**

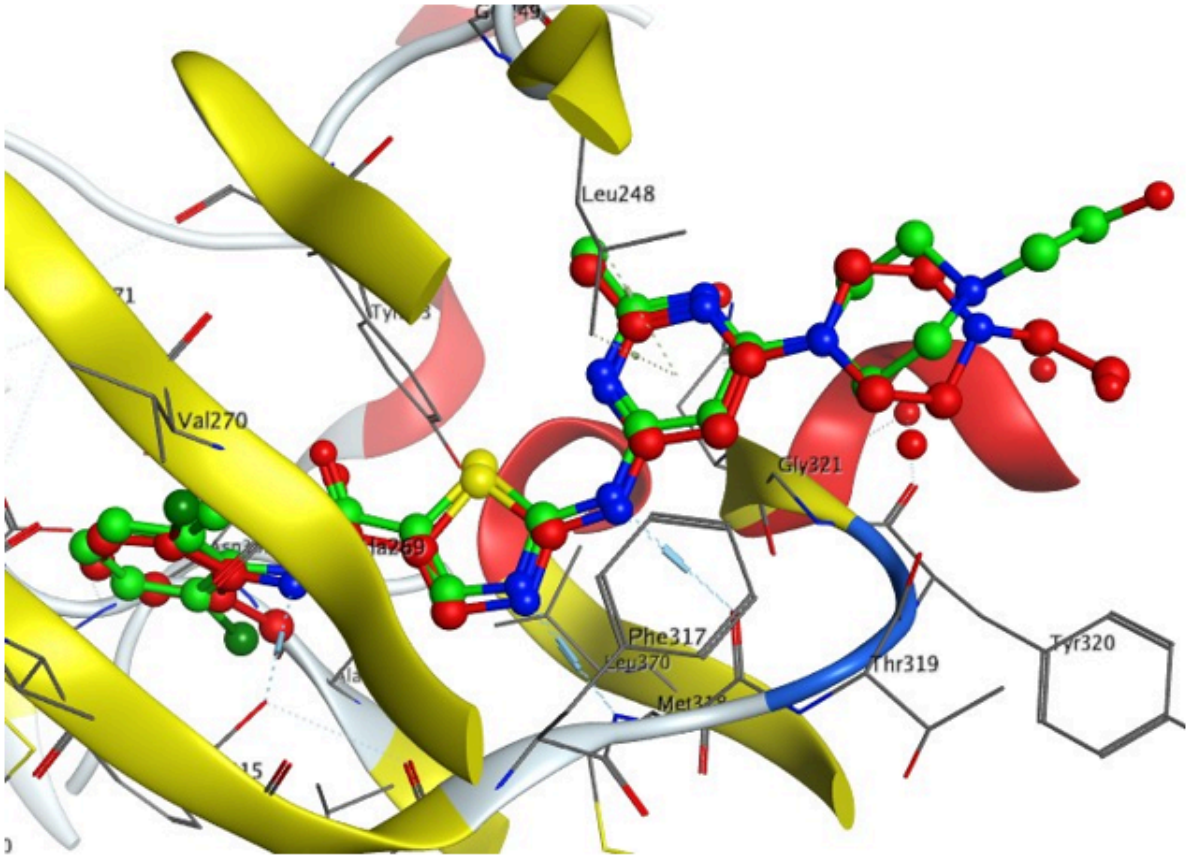

Figure 7

3D Docking pose of 1N1 ligand insight PTK receptor for validation.

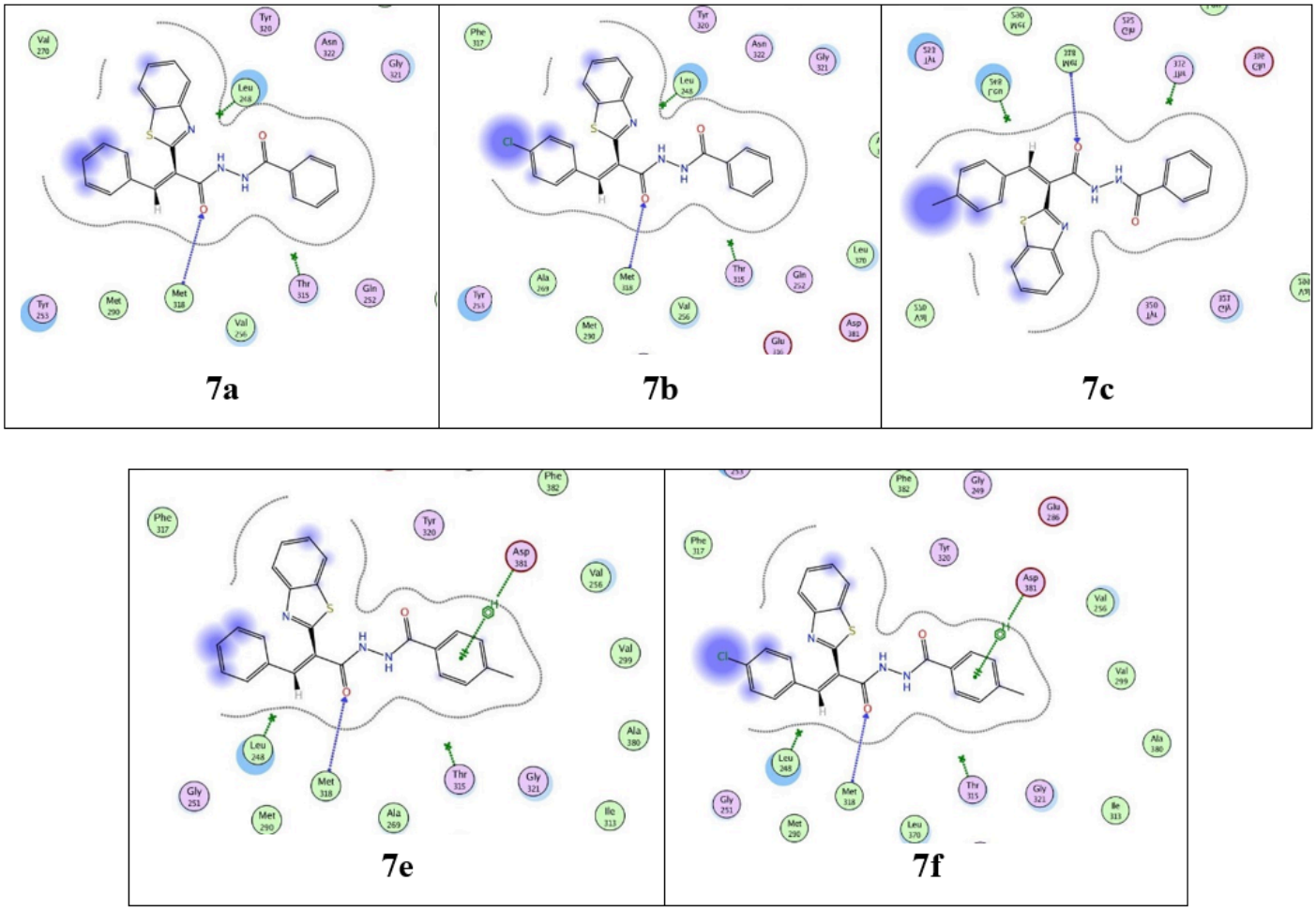

Figure 8

2D Docking poses for **7a-c**, **7e** and **7f** compounds in the binding site of PTK receptor (PDB ID: 2GQG)

Supplementary Files

This is a list of supplementary files associated with this preprint. Click to download.

- Schemes.docx